Journal of Molecular Graphics and Modelling 142 (2026) 109214

Contents lists available at ScienceDirect

Journal of Molecular Graphics and Modelling

journal homepage: www.elsevier.com/locate/jmgm

Structural preferences and multiple bonding interactions in hetero-*closo*-dodecaborates of group-14 elements – A theoretical study

Brindha Veerappan, Krishnamoorthy Bellie Sundaram *

Department of Chemistry (SF), PSG College of Arts and Science, Coimbatore, Tamil Nadu, 641014, India

ARTICLE INFO

Keywords:
$[EB_{11}H_{11}]^{2-}$
$[(EB_{11}H_{11})_2]^{2-}$
DFT-D3
Group-14
Stanna-*closo*-dodecaborate

ABSTRACT

The geometric and electronic structural features of group-14 hetero-*closo*-dodecaborates such as monomers $[HEB_{11}H_{11}]^-$, $[EB_{11}H_{11}]^{2-}$ [E = C (**1a**), Si (**2a**), Ge (**3a**), Sn (**4a**) and Pb (**5a**)] and dimers $[(EB_{11}H_{11})_2]^{2-}$ [E = C (**1**), Si (**2**), Ge (**3**), Sn (**4**) and Pb (**5**)] analyzed using density functional theory (DFT) method at BP86/Def2-TZVP level of theory. The structural features such as the geometry, metrical parameters and bonding interactions are theoretically studied. The dispersion correction method has been used to get more insight which improves the metrical parameter of group-14 elements towards experimental parameters. The electronic structure of the clusters has been studied using frontier molecular orbital analysis (FMO). It shows the group-14 elements electronic contribution and possible electron delocalization between the cages to stabilize the dimeric clusters. DFT (BP86/Def2-TZVP) calculations on the clusters confirm the thermal stability of the newly modelled dimeric clusters (**2**–**5**) which could have diverse applications. The ^{13}C, ^{1}H, ^{29}Si, and ^{11}B nmr chemical shift values computed at DFT (BP86/Def2-TZVP) level are highly useful in identifying and assigning the individual atoms of the monomeric and dimeric clusters. From the global reactivity descriptors and local descriptors analysis, an identification of reactive sites with respect to electrophilic and nucleophilic centers of the reactant has been reported.

1. Introduction

Multiple bonding interactions between group 14 elements have a unique electronic structure and bonding [1–5] which attracts most of the theoretical researchers especially through the density functional theory (DFT) method [6–8]. The bonding interactions of RE/ER [(/→ -, =, ≡), (E = C, Si, Ge, Sn, Pb)] molecules are studied by Shigeru Nagase et al. [9] The heavier group multiple bonds are calculated by using Grimme's dispersion correction D3 method [10]. Icosahedral heteroborates are the kind of Lewis acid-base in which the electrophilicity or nucleophilicity of the clusters mainly depends upon the heteroatoms [11,12]. Boron is a special kind of element that is capable of forming extended binary hydrides, called boranes. This precise species was discovered by Alfred Stock in 1912 [13]. In contrast to hydrocarbons, boranes avoid the formation of chain structures and clearly prefer the formation of polyhedral clusters to overcome the electron deficiency. It can form 2c-2e, 3c-2e, and 4c-2e bonding. This architecture of boranes was proposed by Lipscomb in 1963, and the Nobel Prize was awarded to him for his excellent work on explaining the bonding in these boranes in 1976 [14–16]. Icosahedral borates $[B_{12}H_{12}]^{2-}$ are the twelve vertices of BH units exhibiting perfect Ag symmetry, these dianionic *closo*-dodecaborates arise from the symmetric arrangement of electrons throughout the molecular orbitals of the 12 vertices. Icosahedral borate structures are a kind of three-dimensional configurations made up of triangular B-B-B units. The clusters in this category possess different bonding characteristics compared to typical boron cluster compounds. These clusters exhibit sigma aromaticity or three-dimensional aromaticity due to the spatial delocalization of electron density. The delocalization of two surplus electrons in a dianionic center contributes stability to the sigma bonds of the entire cage, resulting in distinctive steric and electronic properties [17–19]. The heteroatom present in the apical vertex causes slight distortion in Ag symmetry. These distorted icosahedral hetero--*closo*-dodecaborate clusters possess very unique structural characteristics. The Todd group found the first organometallic derivative of dianionic dodecaborate in 1992 [20]. The lone pair electrons at the tin vertex impart Lewis acidity to the stanna-*closo*-dodecaborates, resulting in reactivity towards Lewis bases. It functions as a strong sigma donor and a notable π acceptor, which contributes to ligation, thermodynamic

* Corresponding author.
E-mail address: bskimo@yahoo.co.in (K. Bellie Sundaram).

https://doi.org/10.1016/j.jmgm.2025.109214
Received 21 August 2025; Received in revised form 29 October 2025; Accepted 3 November 2025
Available online 5 November 2025

trans influence, and so forth [17,18]. These icosahedral clusters have been used in boron neutron capture therapy (BNCT), HIV inhibitors, solid state electrolytes, super acids, ligation and etc. [21–33].

Hetero-*closo*-dodecaborate (C, Si, Ge, Sn and Pb) can possess outstanding superionic conductivity, especially above the transition temperatures at which they occur. These anionic *closo*-dodecaborates are found in salts like $LiCB_{11}H_{12}$, $NaCB_{11}H_{12}$ and $Li_2PbB_{11}H_{11}$ which have excellent ionic conductivity and frequently surpass that of liquid electrolytes. At high temperatures, the dodecaborate structure of these salts changes, causing phase transitions that improve superionic conductivity. By removing the possibility of leaks and combustible components, solid-state electrolytes provide a safer substitute for liquid electrolytes. Hetero-*closo*-dodecaborate salts enhance ionic conductivity may contribute to batteries increased energy density. Due to their strong ionic conductivity, better cycle performance, long life and possibility for property tuning, hetero-*closo*-dodecaborates show promise as a novel class of solid-state electrolytes for rechargeable batteries. The goal of ongoing research is to optimize them for real-world use in next-generation batteries and increase their stability, especially at room temperature [26–29].

Boron drugs are specifically designed to target the tumor cells of the patient. The drugs are administered via intravenously, the beam of slow neutrons passes. Boron atoms have the better cross section to capture the neutron particles, then dissociate into lithium ions and high energy alpha particles. It has high linear energy transfer (LET), which is a measure of biological effectiveness of radiation in a more localized manner. So, it can specifically kill the tumor cells, with the minimum damage of healthy cells present in the adjacent areas. Currently, Boron delivery agent researchers are fueling continuous creativity towards better activity and clinical trials with minimum damage [23–26].

The local descriptor and global reactive descriptors are key factors to determine the chemical nature of the system [34–36]. The amphiphilic nature is that the system has both nucleophilic and electrophilic nature which can also be calculated through computational methods [37–39]. This factor is mainly determined by Fukui functions, the global reactive descriptors such as chemical potential (μ), hardness (Ƞ), softness (S) and electrophilicity (ω). These descriptors can be calculated by using DFT method [38,40].

The chemical softness and hardness play a major role in the behavior of the system, this concept first introduced by Robert S. Mulliken at 1952 [41]. Then Hard and Soft Acid Base (HSAB) principle evolved by Pearson postulates. The absolute hardness was introduced by Pearson and Parr. Then Pearson published maximum hardness principle MHP, these two MHP and HSAB are used for the hardness and chemical potential. The Koopmann's theorem mainly used to derive the global reactive descriptors [42]. According to Koopmann's theorem, we can calculate the adiabatic ionization potential (AIP) and vertical ionization potential (VIP). The first ionization energy is derived from the highly occupied molecular orbitals (HOMO), the negative value of the highly occupied molecular orbital's energy plus the electrostatic potential energy of the electron removed from the system. Similarly, we can calculate the ionization potential (IP) average of the highly occupied molecular orbitals (HOMO) of the neutral system (N) and the lowest unoccupied molecular orbitals (LUMO) of the cationic system (N-1) [43].

A dimeric cluster of group-14 icosahedral geometry is reported in 2015 by Wesemann et al.,. The first synthesized hetero-*closo*-dodecaborate dimer is $[Bu_3MeN]_2$ $[(GeB_{11}H_{11})_2]$, a colourless crystalline solid synthesized by the oxidation of germa-*closo*-dodecaborate using iodine and ferroceniumhexafluorophosphate. The dimer is dianionic in nature with the structural formula $[(GeB_{11}H_{11})_2]^{2-}$ [44]. Here we have studied the monomers **1a-5a** and their corresponding dimers **1**–**5** using the DFT method to analyze their molecular structural features, stability and bonding interactions (Scheme 1). Computational chemistry techniques are being used as valuable tools to help with both the modeling of novel compounds and to study the complete structural characterization of existing compounds [45–50]. The following approaches were used to study each of the clusters: the geometry optimization by DFT method at BP86/Def2-TZVP level, molecular orbital analysis, frequency computation, nmr property calculation and reactivity descriptor analysis.

2. Computational details

The hetero-*closo*-dodecaborates are optimized by using BP86/Def2-TZVP level and the interactions are studied by D3BJ method. All of the density functional theory computations in this work were done using ORCA software developed by F. Neese and colleagues [51]. From the Vosko-Wilk-Nusair parameterization [52], the Becke 88 gradient correction for exchange and Perdew 86 correlation inside the local density approximation (LDA) were applied [53–55]. The DFT functional BP86 highly favors the theoretical values with experimental values in metallaboranes [12,56–58]. For each clusters, the Def2-TZVP (triple zeta valence with polarization function) basis set with ZORA (zeroth order regular approximation) was employed. TightSCF convergence requirements were used for all calculation [59]. The bonding interactions of group-14 elements are analyzed by using DFT-D3 method. The Grimme's dispersion correction D3 [60] with BJ (Beck-Johnson) damping [61–63] has been used to approach the closer value of experimental values for the heavy atom system [9,10]. An electron localization function (ELF) analysis done by using ORCA and Multiwfn analyzer. Using the ORCA software's EPRNMR module, the DFT-optimized geometries were utilized to compute nmr parameters such as chemical shifts and shielding constants [64]. The tetramethylsilane (TMS) has been used as reference compound, for computing ^{1}H and ^{13}C nmr chemical shift values [65]. The calculated ^{11}B nmr chemical shift values were translated to the standard BF_3. OEt_2 scale using the experimental value of +16.6 ppm for B_2H_6, with B_2H_6 serving as the major reference point [65,66]. The idea of generalized philicity was presented by Chattaraj et al. It includes information on the electrophilic/nucleophilic power of a specific atomic location in a molecule, as well as nearly all of the previously known various global and local reactivity and selectivity characteristics [67,68]. Further, local descriptors on cluster systems are also explored through DFT method. The binding site of atomic hydrogen on silicon clusters using the local descriptor Fukui Functions [69] and they found the criteria of "maximum matching" between the Fukui functions to predict the best interaction between small (Si_2-Si_6) silicon clusters to form larger (Si_4-Si_8) ones [70]. DFT methods have already been used to find out stable clusters and molecules in the potential energy surface, by kick-Fukui method [71]. The stable global minimum

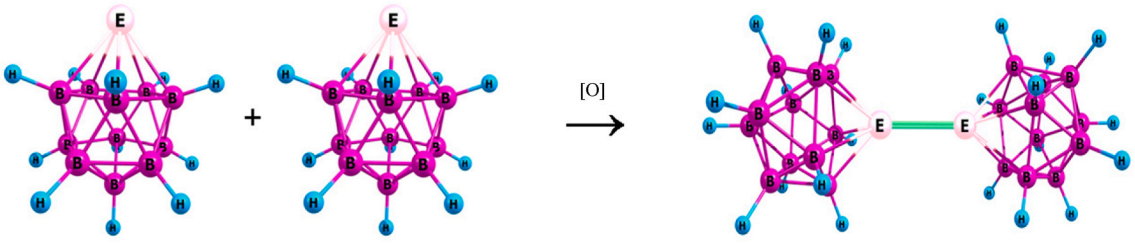

Scheme 1. The schematic diagram representing the molecules studied [E = C (1a), Si (2a), Ge (3a), Sn (4a), Pb (5a)].

structures of $Na(Si_{5-n}(BH)_n)-$ and $Si_{5-n}(BH)_n^{2-}$ (n = 0–5) cluster systems are explored successfully using DFT method by substituting $NaSi_5^-$ and Si_5^{2-} for B–H units [72].

3. Results and discussion

3.1. Geometrical structure

The geometrical structures of the group-14 clusters are studied by

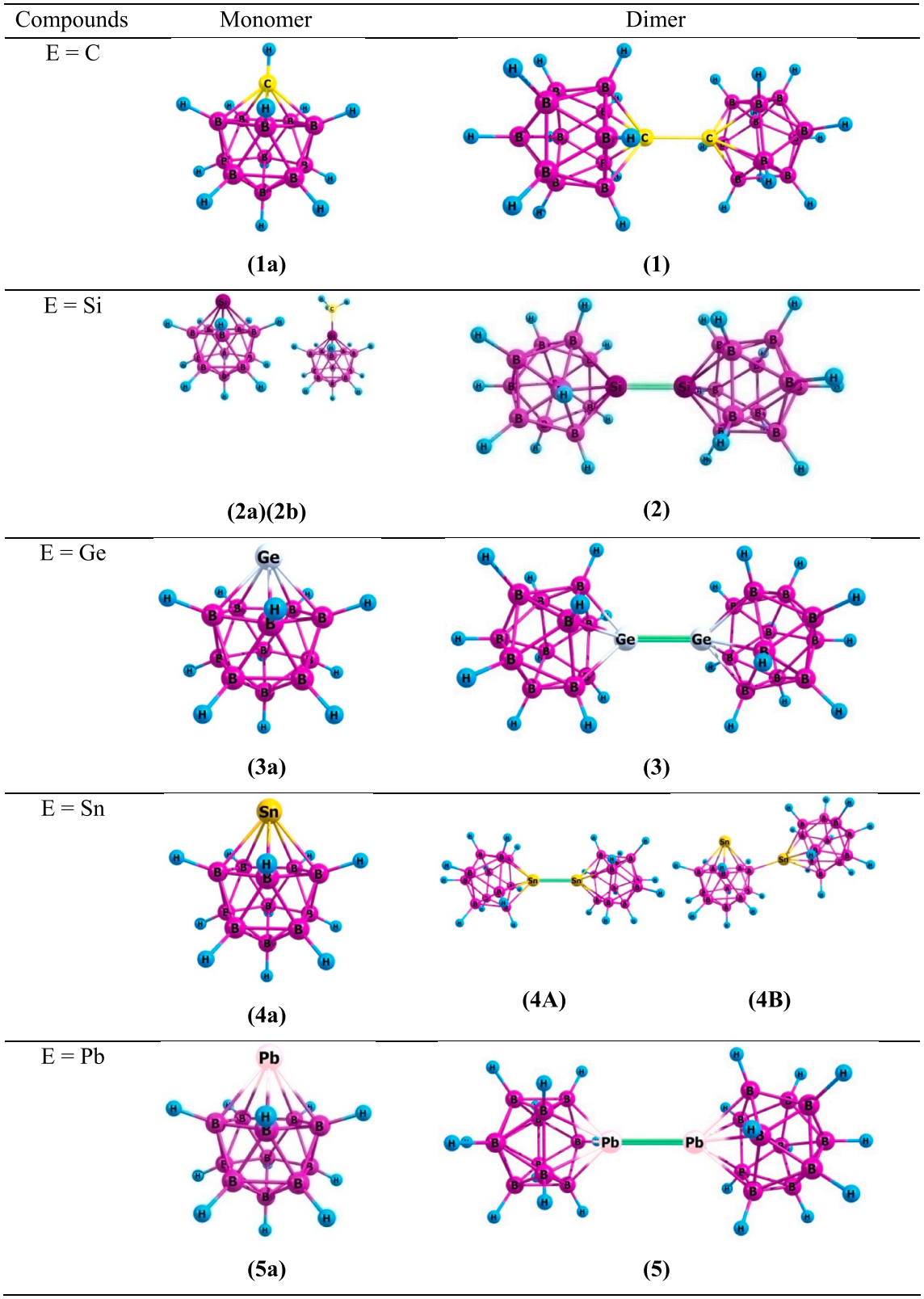

Fig. 1. DFT optimized geometries of group-14 hetero-*closo*-dodecaborate monomers (**1a – 5a**) and dimers (**1–5**) at BP86/Def2-TZVP level.

using BP86/Def2-TZVP level. The optimized geometries are given in Fig. 1. We have optimized monomers and its respective dimers of the group-14 *closo*-dodecaborates. The DFT (BP86/Def2-TZVP) computed metrical parameters and dispersion corrected values of heteroborate monomers (**1a-5a**) are provided in Table S1 and Table S2 respectively. Similarly the DFT (BP86/Def2-TZVP) computed metrical parameters and dispersion corrected values of heteroborate dimers (**1**–**5**) are provided in Table S3 and Table S4 respectively. The bonding distance of E (C, Si, Ge, Sn and Pb) and B atoms are around 1.7091 Å for $[HCB_{11}H_{11}]^-$ (**1a**), 2.1346 Å for $[SiB_{11}H_{11}]^{2-}$ (**2a**), 2.0326 Å [2.0241 Å] for $[MeSiB_{11}H_{11}]^{1-}$ (**2b**) [73], 2.2204 Å for $[GeB_{11}H_{11}]^{2-}$ (**3a**), 2.4029 Å [2.389 (3) Å] [74] for $[SnB_{11}H_{11}]^{2-}$ (**4a**) and 2.4917 Å for $[PbB_{11}H_{11}]^{2-}$ (**5a**). The increasing order of bond length is **1a < 2a < 3a < 4a < 5a < 2b**, the increasing order depends upon the increasing the radii of group-14 elements and interatomic repulsions between B and group-14. The increasing order of bond interactions between E and B atoms using D3BJ method is 1.7061 Å (**1a**) < 2.1307 Å (**2a**) < 2.2143 Å (**3a**) < 2.3973 Å [2.389 (3) Å] (**4a**) < 2.4822 Å (**5a**) < 2.0276 Å [2.0241 Å] (**2b**). Both DFT-D3 calculated and x-ray crystal structure *E*-B bond distance of $[MeSiB_{11}H_{11}]^{1-}$ (**2b**) is 2.02–2.03 Å and $[SnB_{11}H_{11}]^{2-}$ (**4a**) is 2.38–2.40 Å. The DFT-D3 calculated cage vertical distances [CVD] are 3.2286 (**1a**) < 3.9071 (**2a**) < 4.0052 (**3a**) < 4.2298 (**4a**) < 4.3346 (**5a**), the CVD values are gradually increasing from carborate to plumbaborate cage. The dispersion correction method (D3BJ) improves the bonding distances, which are closer to experimental values. The bond angles of B1-E-B2 are 62.834° (**1a**) > 54.904 [54.488] ° (**2b**) > 50.578° (**2a**) > 48.974° (**3a**) > 45.502 [45.380] ° (**4a**) > 43,998° (**5a**). The DFT-D3 method B1-E-B2 bond angles are 62.849 (**1a**) > 54.934 [54.488] (**2b**) > 50.576 (**2a**) > 48.976 (**3a**) > 45.522 [45.380] (**4a**) > 44.043 (**5a**). The cluster (**2b**) and (**4a**) have a good agreement with an experimental value [73,74].

The DFT computed dimeric clusters are $[(CB_{11}H_{11})_2]^{2-}$(**1**), $[(SiB_{11}H_{11})_2]^{2-}$(**2**), $[(GeB_{11}H_{11})_2]^{2-}$(**3**), $[(SnB_{11}H_{11})_2]^{2-}$(**4A**), $[(SnB_{11}H_{10})\ (SnB_{11}H_{11})]^{3-}$(**4B**) and $[(PbB_{11}H_{11})_2]^{2-}$(**5**) have E/E bonding interactions with 1.5535, 2.3290, 2.4048, 2.7377 and 2.8687 Å for the clusters (**1**–**5**) respectively. The dispersion corrected E/E interactions are 1.5386, 2.2955, 2.3715, 2.6986 and 2.8236 Å. An experimental values of the E/E bond of Germa-*closo*-dodecaborate dimer $[Bu_3MeN]_2$ $[(GeB_{11}H_{11})_2]$ is 2.329 (1) Å, which is very closer to the DFT-D3 computed value of $[(GeB_{11}H_{11})_2]^{2-}$ (**3**) is 2.3715 Å, the remaining compounds are not synthesized [44]. So, we have compared an experimental value of the related compounds for the clusters (**1**), (**2**), (**4A**), (**4B**) and (**5**). The C-C interaction of cluster (**1**) is 1.5386 Å which similar to the alkanes C-C bond distance around 1.540 Å [75], confirming the single bond nature. DFT computed Si=Si bond length of 2.2955 Å is similar to the various disilene distance 2.304 (2) Å of 1-methyl-2--phenyl-1,2-disila-*closo*-dodecaborane (12) [(PhSi) (MeSi)$B_{10}H_{10}$] [76], the distance 2.2294 (11) of $[L_2Si{=}SiL_2]$ (L = :C [N (2,6-$Pr^i_2C_6H_3$)CH]$_2$) [77], 216 p.m. or 2.1600 Å presents in $(Mes)_2Si{=}Si(Mes)_2$ [Mes – mesityl group (C_6H_2-2,4,6-Me_3)] [78,79]. The DFT-D3 and DFT computed Sn=Sn double bond distance 2.6986 and 2.7377 Å is very close to the stannylene or distanene (Sn=Sn) double bond 2.6683 (10) Å presents in $(^tBu_2MeSi)_2Sn{=}Sn(SiMe^tBu_2)_2$ [80,81], and 2.702 in $((Me_3Si)_3Si)_2Sn{=}Sn(2,4,6\text{-}Me_3\text{-}C_6H_2)_2$ [84]. The experimentally available structure for stannaborate is $[(SnB_{11}H_{11})\ (SnB_{11}H_{10})]^{3-}$ (**4B**) [44], shown in Fig. 2 and the two stannaborate clusters are inter-connected by 'Sn-B' bonding with 2.2877 Å inter atomic distance. The dispersion corrected (D3BJ) 'Sn-B' bond distance is 2.2445 Å. Both of these DFT and DFT-D3 Sn-B distance is smaller than the usual Sn-B bonds in our monomers and experimental structures [12,74]. The DFT-D3 and DFT computed Pb=Pb bond length of 2.8236 Å and 2.8687 Å is similar to the Pb=Pb bond length 2.833 Å of L:Pb=Pb:L, 2.844 Å of Ph_3Pb-$PbPh_3$ and 2.903 Å of $Si(SiMe_3)_3MesPb{=}PbSi(SiMe_3)_3Mes$ (Mes = 2, 4, 6 - trimethylphenyl) [9].

The B1-E1-E1 angles are gradually increasing from the left to right of the C to Pb series, 119.485° (**1**) < 128.660° (**2**) < 130.149° [128.095°] (**3**) < 134.409° (**4A**) < 137.629° (**5**). The cluster (**3**) has closer value with experimental values. The E1-B1-E2 bond angle of cluster (**4B**) is 177.466°. All the DFT and dispersion corrected DFT-D3 binding interactions, bond length and bond angles are in good agreement with experimental values and related experimental values (Table S3 and S4).

3.2. Chemical descriptors

The chemical descriptors are the indicators of the molecule nature such as reactivity and reactive center. The frontier molecular orbitals (FMO) of the clusters studied are provided in Figure SF3-Figure SF5. Those are divided into two categories, local descriptors like highly occupied molecular orbitals (HOMO), lowest unoccupied molecular orbitals (LUMO), energy gap (ΔE) and global reactive descriptors like chemical potential (μ), hardness (Ƞ), softness (S), electrophilicity (ω), dipole moment, ionization potential (I_P), electron affinity (E_A). These parameters are calculated by using E_{HOMO} and E_{LUMO}. All these descriptors are the major key factor for identifying the natures of the clusters. These descriptors are derived by using Koopmann's theorem.

3.2.1. Local descriptors

We have computed (Table 1) the descriptors for monomers (**1a, 2a, 2b 3a, 4a** and **5a**) and dimers (**1, 2, 3, 4A, 4B** and **5**). The energy gap determines the reactivity and kinetic stability of the geometry, energy of the group-14 monomers are around 3.8368–6.4526 eV. The energy gap range of group-14 dimer is 1.5361–6.3217 eV with highest $E_{LUMO\text{-}HOMO}$ energy gap values of 6.3217 eV for carborate dimer cluster **1**. The increasing order of energy gap for monomer is **5a < 4a < 3a < 2a < 1a** and the dimer is **5 < 4A < 4B < 3 < 2 < 1**. The increasing order shows that the size of the group-14 element increases the energy gap of the

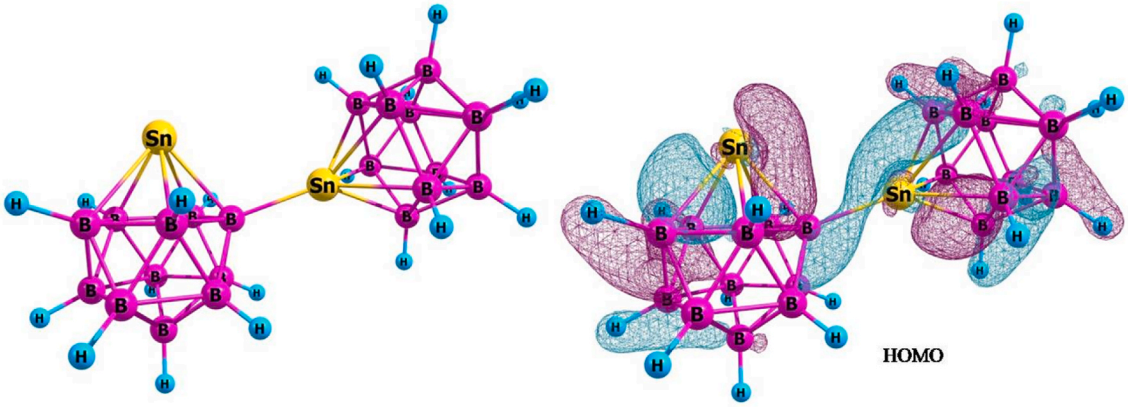

Fig. 2. DFT optimized geometry of $[(SnB_{11}H_{11})\ (SnB_{11}H_{10})]^{3-}$ (**4B**) cluster at BP86/Def2-TZVP level.

Table 1
DFT calculated chemical descriptors (eV) of the monomers (**1a-5a)** and dimeric clusters (**1**–**5)** at BP86/Def2-TZVP level.

Cluster	1a	1	2a	2	3a	3	4a	4 A	4 B	5a	5
HOMO (eV)	−3.3197	−0.9054	2.3009	−1.4080	1.9679	−1.2635	1.7134	−0.9958	2.7506	1.9674	−0.7430
LUMO (eV)	3.1329	5.4163	6.7607	3.6702	6.8277	3.0466	5.9550	1.8011	6.8949	5.8040	0.7931
$E_{LUMO\ -\ HOMO}$	6.4526	6.3217	4.4598	5.0782	4.8598	4.3101	4.2416	2.7969	4.1443	3.8368	1.5361
Chemical potential(μ)	−0.0934	2.2555	4.5308	2.2622	4.3978	1.8116	3.8342	0.4026	4.8228	3.8858	0.0251
Hardness(η)	3.2263	3.1609	2.2299	2.5391	2.4299	2.1551	2.1208	1.3985	2.0722	1.9184	0.7681
Softness (S)	0.3100	0.3164	0.4485	0.3938	0.4115	0.4640	0.4715	0.7151	0.4826	0.5213	1.3019
Electrophilicity(ω)	0.0014	0.8047	4.6029	1.0077	3.9797	0.7614	3.4659	0.0580	5.6122	3.9354	0.0004
Dipole Moment (Debye)	2.65	0.00	0.42	0.03	5.49	0.07	9.14	0.11	8.38	14.11	0.17
Ionization potential(eV)	3.3197	0.9054	−2.3009	1.4080	−1.9679	1.2635	−1.7134	0.9958	−2.7506	−1.9674	0.7430
Electron Affinity (eV)	−3.1329	−5.4163	−6.7607	−3.6702	−6.8277	−3.0466	−5.9550	−1.8011	−6.8949	−5.8042	−0.7931

clusters decreases.

Fukui function has been used to calculate the local descriptors and reactivity sites. Hirsh field analysis lead to the local philicity of the system from which we can determine either it is nucleophilic, electrophilic, neutral or amphiphilic in nature. The following equations (1)–(3) have been used to calculate nucleophilic, electrophilic and radical attack [38].

$$f_k^+ = q_k(N+1) - q_k(N) \quad 1$$

$$f_k^- = q_k(N) - q_k(N-1) \quad 2$$

$$f_k^o = [q_k(N+1) - q_k(N-1)] / 2 \quad 3$$

The dimerization of germa-*closo*-dodecaborate gives the dimeric 'Ge=Ge' bonded $[(GeB_{11}H_{11})]^{2-}$ (**3**) cluster. But, in the case of stanna-*closo*-dodecaborate produces the 'Sn-B' bonded $[(SnB_{11}H_{11})(SnB_{11}H_{10})]^{3-}$ (**4B**) cluster. The quantum chemical computation favors the remaining group-14 dimeric product. The stanna-*closo*-dodecaborate computation possess the favorable results for both the 'Sn=Sn' (**4A**) and 'Sn-B' (**4B**) bonded cluster system. But, the energy gap for the 'Sn-B' system is 4.13 eV with 8.55 Debye dipole moment and 2.7920 eV for the 'Sn=Sn' bonded system. The energy difference for these two systems is around 1.3 eV. So, we have done Fukui function analysis to confirm the product formation.

The calculation of electrophilic Fukui function (f_k^+), nuclophilic Fukui function (f_k^-) and neutral Fukui function (f_k^o) through N-1, N+1 and N systems. The calculation shows that the f_k^-, f_k^o favours the B2 vertex with −0.0190, −0.0197 and $f_k{}^+$ favours B4 vertex with −0.0197. So, B2 and B4 vertex is electrophilic and nucleophic respectively, in nature. So, this analysis highly favours the 'Sn-B' bonded $[(SnB_{11}H_{11})(SnB_{11}H_{10})]^{3-}$ (**4B**) cluster formation. But, in the tin vertex, the calculations gives f_k^+, f_k^- and f_k^o −0.5402, −0.2689 and −0.4046. Hence, tin vertex is highly nucleophilic in nature and less electrophilic nature. So, the 'Sn=Sn' (**4A**) bonded dimeric cluster is less favored.

3.2.2. Global reactive descriptors

The global reactive descriptors are calculated by using below equations (4)–(8), the equation solved by using frontier molecular orbital HOMO and LUMO [45]. The DFT computed chemical descriptors are given in Table 1.

$$\text{Electronegativity} = -\frac{1}{2}(E_{LUMO} + E_{HOMO}) \quad 4$$

$$\text{Global Chemical Potential } (\mu) = \frac{1}{2}(E_{LUMO} + E_{HOMO}) \quad 5$$

$$\text{Global Hardness } (\eta) = \frac{1}{2}(E_{LUMO} - E_{HOMO}) \quad 6$$

$$\text{Global Softness}(S) = 1/\eta \quad 7$$

$$\text{Global Electrophilicity } (\omega) = \frac{\mu 2}{2\eta} \quad 8$$

Chemical potential (μ) of the carboratecluster **(1a)** and plumbaborate **(5)** has very lower values −0.0934 and 0.0251, the lowest value obtained due to higher nucleophilicity of the cluster. The monomers have the higher (μ) value than the dimers except carborate system. It determines that the dimers are highly nucleophilic in nature than the monomers; the heavy group clusters Sn and Pb dimers are good at this criterion.

Hardness (η) determines the overall stability of the clusters. The harness increases the stability of the system increases. The hardness of the carborates (**1, 1a**) has higher value around 3.2263 to 3.1609 than the remaining group-14 clusters. But, in the case of electrophilicity (**ω**), the carborates **(1, 1a)** have lower value than the remaining group-14 clusters. The hardness values are gradually decreases from the silaborates to plumbaborates except (**4B**).

Softness (S) of the clusters is lower in all geometries except the dimeric plumbaborate (**5**) geometry as 1.3019 eV. The higher softness value indicates that the cluster has the possibility to better reactivity. Similarly, the better reactivity of this cluster is supported by the lower energy gap than the remaining group-14 geometries with less hardness and electrophilicity. Hence, we can find the stability and reactivity of the clusters through hardness (η) and softness (S).

Electrophilicity(**ω**) of the monomeric clusters (**2a, 2, 3a, 4a, 4B** and **5a**) are higher than the dimers except carborates. In the dimeric system, the silaborate only has the considerable electrophilicity value at 1.0077 eV. The dipole moment of the dimeric clusters (**1, 2, 3, 4** and **5**) are almost zero except dimer (**4B)** with 8.3763 Debye dipole moment and the monomers are in the order of 14.1067 **(5a)** > 9.1407 **(4a)** > 5.4925 **(3a)** > 2.6467 **(1a)** > 0.4212 **(2a)**. Among the monomers studied the plumba-*closo*-dodecaborate (**5a)** polar cluster has highest dipole moment (DM) value of 14.11 Debye (D) when compared to the than the remaining group-14 monomeric clusters. According to Koopmann's theorem negative value of HOMO is termed as ionization potential (IP) and negative value of LUMO is termed as electron affinity (EA). The carborate shows the highest IP 3.3197 eV and dimeric plumbaborate shows highest EA -0.7931 eV.

3.3. Polyhedral skeletal electron pair theory (PSEPT) and cluster valence electron (CVE) count

The skeletal electron pair count and electronic structure of the clusters are studied by PSEPT theory [82–84]. The PSEPT and CVE suggests that the icosahedral borate $[B_{12}H_{12}]^{2-}$ cluster has 13 skeletal electron pair (SEP) possess the *closo* geometry, with the general formula of the *closo* geometry $[B_nH_n]^{2-}$ [82].

$$12 \text{ x } 2\ (BH) + 2\ (2e^-) = 26\ e^-s$$

$$26 / 2 = 13$$

$$SEP = (n+1) = (12+1) = 13$$

$n = 12\ (12 - \text{vertex icosahedral geometry})$

Similarly, the group 14 clusters also possess the *closo* geometry with 13 SEP and n = 12. So, the monomers of the group 14 clusters obeys the wades rule, the geometrical formula of the group 14 clusters are $[HCB_{11}H_{11}]^{-}$, $[SiB_{11}H_{11}]^{2-}$, $[GeB_{11}H_{11}]^{2-}$, $[SnB_{11}H_{11}]^{2-}$ and $[PbB_{11}H_{11}]^{2-}$.

$11\ x\ 2\ (BH) + 1\ x\ 3\ (C) + 1\ (1e^{-}) = 26\ \text{electrons}$

$11\ x\ 2\ (BH) + 1\ x\ 2\ (E) + 2\ (2e^{-}) = 26\ \text{electrons}\ (E = Si, Ge, Sn, Pb)$

$26 / 2 = 13$

$SEP = (n + 1) = (12 + 1) = 13$

$n = 12$

Hence, the clusters possess *closo* icosahedral geometry, the structure is slightly distorted at the hetero atom vertex. So, the geometrical structure of the group-14 cluster is distorted icosahedral structure and termed as distorted hetero-*closo*-dodecaborate.

3.4. Bond order

The Mayer bond analysis used to determine the bond order and charge density of the atoms. The E/E bond orders of dimeric compounds are given in Table 2. The bond order of the E/E bond presents in the carborate **(1)** is 1.1633, 0.8227 in silaborate **(2)**, 0.8299 in germaborate **(3)**, −3.3836 for stannaborate **(4A)** and 0.8944 for plumbaborate **(5)** clusters. Hence, the bond order of all clusters proves that the bonding interactions presents in the group-14 clusters except stannaborates. The stannaborate shows that the negative bond order value in DFT (−3.3836) and DFT-D3 (−0.3721) method which could be due to the restriction or bugs in the method/software for this specific system. The bond order values obtained from the DFT-D3 methods are slight lower than the DFT method for C and Si systems. But, in the remaining cases, the *E*-E (Ge, Sn, Pb) bond order is slightly higher than the DFT method. The difference for the Ge cluster is 0.0813 and Sn cluster is 3.0115. The DFT-D3 computed Sn2-B1 bond order of cluster (**4B**) is 0.9361. The Pb cluster is DFT-D3 (1.0439) value is higher than the DFT (0.8944) method. The difference between these two methods proves the D3 method is highly favorable for the heavy atoms.

3.5. Electronic structure

The frontier molecular orbitals (FMO) of the clusters studied are provided in Fig. SF3 - SF5. The highly occupied molecular orbitals (HOMO) of the monomers **(1a-5a) mainly** involve **the electron density located at the boron vertices**. In contrast, in **the lowest unoccupied molecular orbitals (LUMO), electron density is localized at the group 14 elements. In the dimeric clusters, also similar trend continues. In the case of LUMO and LUMO+1 of disilaborate (2) electrons are delocalized over the two *closo* clusters, which is seen in the** picture Fig. SF3 - SF5. The LUMO+1 and LUMO+2 of germaborates **(3)** has electron density over the Ge-Ge bonding. The LUMO+1 and LUMO+2 of stannaborate **(4A)** and plumbaborate **(5)** have the electron density over the *E*-E bond. The HOMO of the cluster (**4B**) shows the electron density over the two *closo* clusters, shown in Fig. 2.

3.6. Electron localization function (ELF) analysis

Electron Localization Function (ELF) Analysis from computations are highly useful I confirming the metal-metal, multiple bonding interactions [56]. The bonding nature using ELF analysis of group 14 elements presents in the dimeric hetero-*closo*-dodecaborates are shown in Fig. 3. The colour bar range is 0–1, the highest electron localization at red and lowest electron localization at dark blue. The electron cloud value below 0.5 shows the low electron density [56]. The carborate has good electron density between two carbon atoms as red colour range 0.9–1. The order of electron cloud density from carbon to lead is carborate < silaborate > germaborate > stannaborate > plumbaborate. But, In the case of stannaborates electron density, the Sn-B density (0.7–0.8 orange) overcomes Sn-Sn electron density (green 0.6). The overall ELF analysis shows very good electron density of group 14 elements for sila-*closo*-dodecaborate dimer (**2**).

3.7. Thermochemistry

The thermochemical calculations of the monomers and dimers through frequency analysis give no imaginary frequency and the obtained optimized geometries also minima in the potential energy surface. The DFT (BP86/Def2-TZVP) computed thermal energy, enthalpy, entropy, Gibbs free energy are given in Table 3. The DFT computed free energy of the dimer-forming reactions, confirming the stable nature of the modelled dimers and supports their viable synthesis.

The energy of the reactions for the dimers are given in Table 4. This energy is derived from the subtracting the total thermal energy (U) of the product and 2 mol of reactants, then the Hartree value is converted to kcal/mol.

Energy of the reaction by using total thermal energy (U),

$$\Delta U = U_{Product} - U_{Reactants} \quad (9)$$

Enthalpy of the reaction,

$$\Delta H = H_{Product} - H_{Reactants} \quad (10)$$

Gibbs free energy,

$$\Delta G = \Delta H - (T \times \Delta S) \quad (11)$$

Gibbs free energy of the reaction,

$$\Delta G = G_{Product} - G_{Reactants} \quad (11a)$$

The borates of silicon and germanium have the energies using total thermal energy is −44.5531 kcal/mol and −22.2138 kcal/mol respectively, which indicates that the reactions are feasible in which germa-*closo*-dodecaborate dimer is an experimentally known cluster. The energy of the reaction for the formation of diplumba-*closo*-dodecaborate is 25.2 kcal/mol. Interestingly for the stanna-*closo*-dodecaborate dimer with Sn=Sn (**4A**) and Sn-B (**4B**) has 2.3835 kcal/mol and 416.9 kcal/mol. The cluster (**4A**) has 2.3 kcal/mol which is lower energy than an experimentally known cluster hetero-*closo*-distannaborate (**4B**) with Sn-B bond [44] and confirming the viability of the modelled cluster hetero-*closo*-distannabotrate (**4A**) with Sn=Sn bonding.

The change in entropy of the reaction, has been calculated using equation (12)

$$2\ [EB_{11}H_{11}]^{2-} \rightarrow [(EB_{11}H_{11})_2]^{2-}$$

Table 2
The E/E bond order of group 14 hetero-*closo*-dodecaborate dimers at BP86/Def2-TZVP level using normal DFT and DFT-D3 method.

Clusters	C		Si		Ge		Sn		Pb	
	DFT	D3	DFT	D3	DFT	D3	DFT	D3	DFT	D3
Mayer	1.16	1.04	0.82	0.77	0.83	0.91	–	–	0.89	1.04

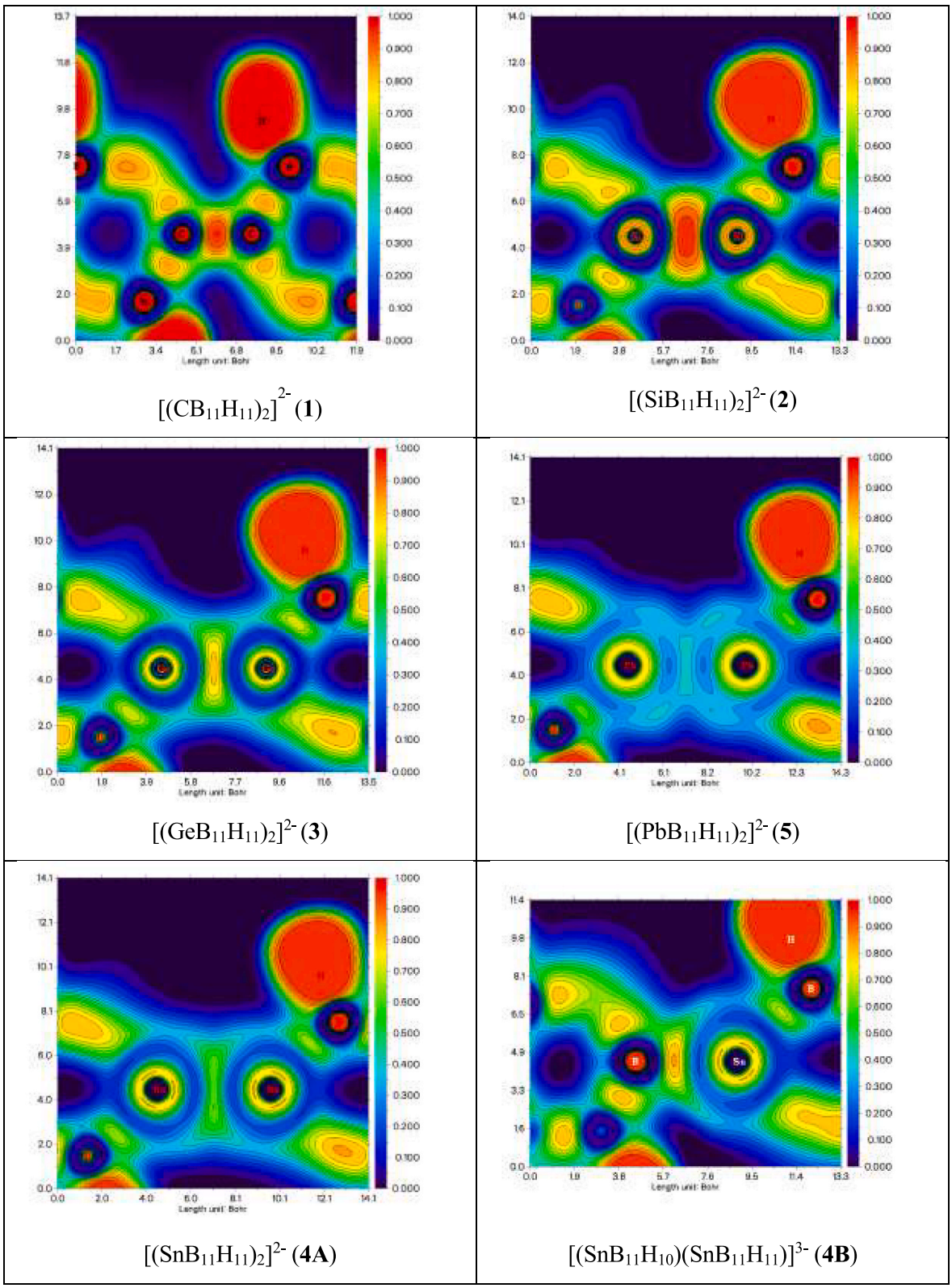

Fig. 3. ELF diagram for the DFT optimized geometries of dimers (**1**–**5**) at BP86/Def2-TZVP level using Multiwfn analyzer.

Two moles of reactant → 1 mol of dimer

$$\Delta S = S_{Product} - S_{Reactant} \quad 12$$

The DFT (BP86/Def2-TZVP) computed entropy of the reaction values for the experimentally known dimers (**3**) and (**4B**) are −0.0207 E h and −0.0232 E h respectively, Table 4. The plumba-*closo*-dodecaborate dimer (**5**) has the slightly higher value −0.0194 Hartrees than the remaining dimers. The change in Gibbs free energy for the dimer forming reaction confirm the more feasible nature of dimers **2, 3, 4A** and **5** and less feasible nature of **1** with 1.2989 Hartrees. From the free energy values of the dimer forming reaction, the following order has been

Table 3
DFT calculated thermochemical properties of group 14 hetero-*closo*-dodecaborate monomers and dimers at BP86/Def2-TZVP level.

Clusters	Total thermal energy (U)	Enthalpy (H)	Entropy (S)	Gibbs free energy (G)
$[HCB_{11}H_{11}]^-$	−318.8699 E h	−318.8689 E h	0.0397 E h	−318.9087 E h
$[SiB_{11}H_{11}]^{2-}$	−569.6334 E h	−569.6324 E h	0.0414 E h	−569.6738 E h
$[GeB_{11}H_{11}]^{2-}$	−2357.3931 E h	−2357.3922 E h	0.0428 E h	−2357.4350 E h
$[SnB_{11}H_{11}]^{2-}$	−494.5461 E h	−494.5452 E h	0.0440 E h	−494.5891 E h
$[PbB_{11}H_{11}]^{2-}$	−473.1383 E h	−473.1374 E h	0.0451 E h	−473.1824 E h
$[(CB_{11}H_{11})_2]^{2-}$	−636.4633 E h	−636.4623 E h	0.0562 E h	−636.5185 E h
$[(SiB_{11}H_{11})_2]^{2-}$	−1139.3379 E h	−1139.3369 E h	0.0621 E h	−1139.3989 E h
$[(GeB_{11}H_{11})_2]^{2-}$	−4714.8216 E h	−4714.8207 E h	0.0649 E h	−4714.8855 E h
$[(SnB_{11}H_{11})_2]^{2-}$	−989.0885 E h	−989.0875 E h	0.0676 E h	−989.1551 E h
$[(SnB_{11}H_{10})(SnB_{11}H_{11})]^{3-}$	−988.4279 E h	−988.4276 E h	0.0648 E h	−988.4924 E h
$[(PbB_{11}H_{11})_2]^{2-}$	−946.2364 E h	−946.2354 E h	0.0708 E h	−946.3063 E h

depicted for the formation of dimer, **2** > **3** > **4A** > **5** > **4B**.

3.8. Spectroscopic properties

The hetero-*closo*-dodecaborate has three types of protons and borons which lead to three types of chemical shifts (δ), upper belt (5 B (1–5) and 5H (1–5)), lower belt (5 B (6–10) and H (6–10)) and apical vertex (B11 and H11). The DFT computed chemical shift values are given in Tables S10–S14. The ^{11}B nmr chemical shifts are resonates in 1:5:5 ratio. Usually upper belt borons and protons has lower chemical shift than lower belt and apical position through the higher shielding effects presents in the upper belt than in the remaining atoms. According to the presence of group-14 heteroatoms, the upper belt obtains higher shielding effect. The difference between the lower belt and upper belt is around 2–4 ppm. When comparing these two belts with apical vertex, the chemical shift of apical position is very high. The apical vertex B and H atoms are highly deshielded, these elements utilize higher resonating energy around 4–10 ppm than the remaining atoms. The DFT (BP86/Def2-TZVP) computed chemical shift for C atom of cluster (**1a)** is 58.74 which is close to the experimental value of 51.5 ppm. An upper belt boron resonates around −21.22 to −21.26 ppm which is close to the experimental value of −16.31 ppm. The lower belt boron resonates around −17.24 to −17.27 ppm which is also close to the experimental value of −13.30 ppm. The apical boron B11 [DFT -11.21 ppm; Experimental −6.90 ppm]. Is less shielded when compared to those of upper best and lower belt boron atoms. The ^{1}H nmr shows that the chemical shift values of hydrogen atoms are in1:5:5 ratio, the proton connected with the C atom resonates at 2.17 ppm which is close to the experimental value of 2.24 ppm [85,86]. Similarly, each monomers (**2a-5a)** and dimers (**1**–**5**) except (**4B)** computed chemical shifts of ^{11}B, ^{1}H resonates like 1:5:5 for monomers and both cages of dimers. The ^{13}C nmr of carborate dimer $[(CB_{11}H_{11})_2]^{2-}$ (**1**) resonates around 86.0 ppm. The silicon atom of the methyl substituted sila-*closo*-dodecaborane (**2b**) The ^{29}Si nmr of experimentally known cluster (**2b**) has been computed at DFT (BP86/Def2-TZVP) level as −36.84 ppm which is close to the experimental value of −28.0 ppm [2,20,73]. The $[(GeB_{11}H_{11})_2]^{2-}$ **(3)** cluster resonates 1:5:5 ratio [44]. In the stannaborate (**4a**) and plumbaborate (**5a**) monomers the ^{11}B nmr shows peaks in the 1:5:5 ratio. The DFT and experimental values are −8.72 [5.1]: 16.23 [−10.6]: 18.14 [−11.9] ppm for **(4a)** and −7.74 [−2.9]: 18.53 [−10.3]: 14.46 [−5.0] ppm for (**5a**) [20], whereas the dimers resonates at −14.0: 21.0: 19.0 and −21.0: 24.0: 17.0 (B11:B6-B10:B1-B5). The boron atoms of $(SnB_{11}H_{10})(SnB_{11}H_{11})]^{3-}$ (**4B)** cluster resonates at −11.36 [−13.6] (B1); −17.59 [−8.0] (B8); −8.57 [−3.6] (B11); −14.83 [−10.0] (B2), −14.92 [−10] (B5); −14.92 [−8.6] (B3), −14.92 [−8.6] (B4); −17.60 [−11.4] (B6), −17.44 [−11.4] (B10), −17.58 [−11.4] (B7), −17.41 [−11.4] (B9); −21.91 to −22.50 [−15.8] (B12-B22) ppm. An experimentally reported ^{11}B nmr ratio is 1:1:1:2:2:2:2:11. But, the ratio of cage **2** in (**4B)** normal icosahedrons 1:5:5 ratio peakas −21.19 (B1-B5): 22.51 (B6-B10): 15.36 (B11) ppm. The apical vertex H11 resonates at 2.447 ppm which is less shielded as expected, than the ^{1}H nmr chemical shifts of the remaining hydrogen atoms of $(SnB_{11}H_{10})(SnB_{11}H_{11})]^{3-}$ (**4B**) cluster [44]. The DFT (BP86/Def2-TZVP) calculated ^{11}B, ^{13}C, ^{1}H and ^{29}Si nmr chemical shift values are helpful in assigning the individual atoms of the monomeric and dimeric clusters.

4. Conclusions

The bonding interactions of hetero-*closo*-dodecaborates (**1a – 5a)** and their dimers (**1**–**5**) are analyzed using density functional theory (DFT) and DFT-D3 method at BP86/Def2-TZVP level of theory. The viable nature of the dimeric hetero-*closo*-dodecaborate clusters (**2**–**5**) are confirmed through DFT computations. Although, normal DFT optimization leads to the closer values towards experimentally obtained bond parameters, inclusion of dispersion correlation suggested by Grimme et al. improves the metrical parameters significantly (~0.04 Å in bond length) towards an experimental value. Further, inclusion of dispersion correction provides the energies more accurately. The DFT computed global and local descriptors have predict correctly the labile nature of the stannaborate dimer (**4A**) with 'Sn=Sn' double bond. Both DFT and experimental studies confirm the more stable nature of the stannaborate dimer (**4B)** with possible Sn-B bonding interaction. The global electrophilicity index (ω) of the monomeric clusters (**2a, 2, 3a, 4a** and **5a)** are higher than the dimers except carborates. DFT (BP86/Def2-TZVP) calculations on the clusters confirm the thermal stability of the newly modelled dimeric clusters (**2**–**5)** which could have diverse applications. ELF analysis confirm the high electron density around, 0.5 to 0.9 range for E = E bond in each dimers except the dimer (**5**). From the free energy values of the dimer forming reaction, the following order, **2 > 3 > 4A > 5 > 4B.,** has been depicted for the formation of dimer. The DFT (BP86/Def2-TZVP) computed spectroscopic values are in good agreement with

Table 4
DFT calculated Energy of the reaction using total thermal energy (U), enthalpy (H), Gibbs free energy (G) and entropy (S) for group 14 hetero-*closo*-dodecaborate dimers at BP86/Def2-TZVP level.

Dimers	ΔU		ΔH		ΔG		ΔS	
	Hartrees	kcal/mol	Hartrees	kcal/mol	Hartrees	kcal/mol	Hartrees	Kcal/mol
1	1.2765	801.0	1.2755	800.4	1.2989	815.1	−0.0232	−14.6
2	−0.0710	−44.6	−0.0721	−45.2	−0.0513	−32.2	−0.0207	−13.0
3	−0.0354	−22.2	−0.0363	−22.8	−0.0155	−9.7	−0.0207	−13.0
4 A	0.0037	2.4	0.0029	1.8	0.0231	14.5	−0.0204	−12.8
4 B	0.6643	416.9	0.6628	415.9	0.6858	430.3	−0.0232	−14.6
5	−0.0401	25.2	0.0394	24.7	0.0585	36.7	−0.0194	−12.2

the experimental values when available or with similar clusters. The ^{13}C, ^{1}H, ^{29}Si, and ^{11}B nmr chemical shift values computed at DFT (BP86/Def2-TZVP) level are highly useful in identifying and assigning the individual atoms of the monomeric and dimeric clusters.

CRediT authorship contribution statement

Brindha Veerappan: Writing – original draft, Methodology, Investigation, Data curation. **Krishnamoorthy Bellie Sundaram:** Writing – review & editing, Supervision, Investigation, Conceptualization.

Declaration of competing interest

The authors declare that they have no known competing financial interests or personal relationships that could have appeared to influence the work reported in this paper.

Appendix A. Supplementary data

Supplementary data to this article can be found online at https://doi.org/10.1016/j.jmgm.2025.109214.

Data availability

No data was used for the research described in the article.

References

[1] P.P. Power, π-Bonding and the lone pair effect in multiple Bonds between Heavier Main Group elements, Chem. Rev. 99 (1999) 3463–3504, https://doi.org/10.1021/cr9408989.

[2] K.W. Klinkhammer, W. Schwarz, Bis(hypersilyl)tin and bis(hypersilyl)lead, two electron-rich carbene homologs, Angew. Chem., Int. Ed. Engl. l34 (1995) 1334–1336, https://doi.org/10.1002/anie.199513341.

[3] H. Zhiyuan, L. Lingyu, J.D.Z. Felix, X. Xiaolian, W.E. Andreas, Y. KaKing, D. Serhiy, V. Jarl Ivar van der, B. Bas, K. Jeremy, Reactivity of a unique Si(I)–Si(I)-Basedη^2-Bis(silylene) iron complex, Inorg. Chem. 61 (30) (2022) 11725–11733, https://doi.org/10.1021/acs.inorgchem.2c01369.

[4] M. Stürmann, W. Saak, K.W. Klinkhammer, M. Weidenbruch, A Heteroleptic (E)-1,2-Diaryl-1,2-disilyl distannene without Donor Stabilization, Zeitschrift. Für. Anorganische. Und, Allgemeine. Chemie. 625 (1999) 1955–1956, https://doi.org/10.1002/(SICI)1521-3749(199912)625:12<1955::AID-ZAAC1955>3.0.CO;2-J.

[5] R. Bashkurov, N. Fridman, D. Bravo-Zhivotovskii, Y. Apeloig, The first planar, not twisted, Distannene −A structural alkene analog, synthesis, isolation and x-ray crystallography characterization, Chem. Eur J. 29 (69) (2023) e202302678, https://doi.org/10.1002/chem.202302678.

[6] P.J. Davidson, D.H. Harris, M.F. Lappert, Subvalent Group 4B metal alkyls and amides. Part I. The synthesis and physical properties of kinetically stable Bis[bis(trimethysilyl)methyl]-germanium(II), -tin(II), and -lead(II), J. Chem. Soc. Dalton Trans. (1976) 2268–2274, https://doi.org/10.1039/DT9760002268.

[7] K.W. Klinkhammer, T.F. Fässler, H. Grützmacher, The Formation of HeterolepticCarbene homologues by Ligand exchange - synthesis of the first plumbanediyl dimer, Angew. Chem. Int. Ed. 37 (1998) 124–126, https://doi.org/10.1002/(SICI)1521-3773(19980202)37:1/2<124::AID-ANIE124>3.0.CO;2-C.

[8] S. Wang, H.J. Li, T.S. Kuo, L.C. Shen, H.J. Liu, Ambiphilic Nature of dipyrrolylpyridine - supported divalent germanium and tin compounds, Organometallics 40 (2021) 3659–3667, https://doi.org/10.1021/acs.organomet.1c00494.

[9] S. Nagase, Multiple bonds between lead atoms and short bonds between transition metals, Pure Appl. Chem. 85 (2012) 649–659, https://doi.org/10.1351/PAC-CON-12-08-04.

[10] J.D. Guo, D.J. Liptrot, S. Nagase, P.P. Power, The multiple bonding in heavier group 14 element alkene analogues is stabilized mainly by dispersion force effects, Chem. Sci. 6 (2015) 6235–6244, https://doi.org/10.1039/C5SC02707A.

[11] S. Körbe, P.J. Schreiber, J. Michl, Chemistry of the carba-*closo*-dodecaborate(−) anion, CB11^{H}12^{-}, Chem. Rev. 106 (2006) 5208–5249, https://doi.org/10.1021/cr050548u.

[12] T. Gädt, L. Wesemann, Stanna-*closo*-dodecaborate chemistry, Organometallics 26 (2007) 2474–2481, https://doi.org/10.1021/om061042k.

[13] A. Stock, O. Maesenez, Reports of the German Chemical Society 45 (3) (1912) 3539–3568, https://doi.org/10.1002/cber.191204503113, boron hydrogens.

[14] W.N. Lipscomb, Boron Hydrides, the Physical Inorganic Chemistry Series, Harvard University, New York, 1963.

[15] W.N. Lipscomb, Bonding in boron hydrides, Pure Appl. Chem. 29 (4) (1972) 493–512, https://doi.org/10.1351/pac197229040493.

[16] N.S. Hosmane, J.A. Maguire, Boron Hydrides, based in part on the article Boron Hydrides by James T. Spencer which appeared in the *Encyclopedia of Inorganic Chemistry*, in: Encyclopedia of Inorganic Chemistry, first ed., John Wiley & Sons, Ltd., 2006 https://doi.org/10.1002/0470862106.ia024. ISBN: 9780470862100.

[17] I.E. Golub, O.A. Filippov, V.A. Kulikova, N.V. Belkova, L.M. Epstein, E.S. Shubina, Thermodynamic hydricity of small borane clusters and polyhedral *closo*-Boranes, Molecules 25 (12) (2020) 2920, https://doi.org/10.3390/molecules25122920.

[18] J. Aihara, Three-dimensional aromaticity of polyhedral boranes, J. Am. Chem. Soc. 100 (11) (1978) 3339–3342. https://pubs.acs.org/doi/10.1021/ja00479a015.

[19] R.B. King, Three-Dimensional aromaticity in polyhedral boranes and related molecules, Chem. Rev. 101 (5) (2001) 1119–1152, https://doi.org/10.1021/cr000442t.

[20] R.W. Chapman, J.G. Kester, K. Folting, W.E. Streib, L.J. Todd, Synthesis and chemistry of $B_{11}H_{11}Sn^{2-}$ and its germanium and lead analogs. Crystal structure of $[B_{11}H_{11}SnCH_3]PPh_3CH_3.CH_2Cl_2$, Inorg. Chem. 31 (6) (1992) 979–983, https://doi.org/10.1021/ic00032a011.

[21] T. Wutz, F. Diab, L. Wesemann, Synthesis and coordination chemistry of a P-Sn-chelating ligand based on stanna-*closo*-dodecaborate, Eur. J. Inorg. Chem. 2017 (2017) 4645–4652, https://doi.org/10.1002/ejic.201700471.

[22] M.A. Fox, T.B. Marder, L. Wesemann, DFT studies of the σ-donor/π-acceptor properties of $[SnCB_{10}H_{11}]^-$ and its relationship to $[SnCl_3]^-$, CO, PF_3, $[SnB_{11}H_{11}]^{2-}$, $SnC_2B_9H_{11}$, and related $SnC_2B_nH_{n+2}$ compounds, Can. J. Chem. 87 (1) (2009) 63–71, https://doi.org/10.1139/v08-081.

[23] M.F. Hawthorne, A. Maderna, Applications of radiolabeled boron clusters to the diagnosis and treatment of cancer, Chem. Rev. 99 (1999) 3421–3434, https://doi.org/10.1021/cr000001+. Published on the Web Nov. 13, 1999. Chem Rev 100(3) (2000) 1165.

[24] M.F. Hawthorne, S.S. Jalisatgi, A.V. Safronov, H.B. Lee, J. Wu, Chemical Hydrogen Storage Using Polyhedral Borane Anions and aluminum-ammonia-borane Complexes, International Institute of Nano and Molecular Medicine, University of, Missouri, United States, 2010, https://doi.org/10.2172/990217.

[25] W.H. Jin, C. Seldon, M. Butkus, W. Sauerwein, H.B. Giap, A review of Boron Neutron capture therapy: its history and Current challenges, International Journal of Particle Therapy 9 (2022) 71–82, https://doi.org/10.14338/IJPT-22-00002.1.

[26] L. Pazderová, E.Z. Tüzün, D. Bavol, M. Litecká, L. Fojt, B. Grűner, Chemistry of carbon-substituted derivatives of cobalt Bis(dicarbollide)(1−) ion and recent progress in boron substitution, Molecules 28 (2023) 6971, https://doi.org/10.3390/molecules28196971.

[27] S.H. Payandeh, R. Asakura, P. Avramidou, D. Rentsch, Z. Łodziana, R. Černy, A. Remhof, C. Battaglia, Nido-Borate/Closo-Borate mixed-anion electrolytes for All-SolidState batteries, Chem. Mater. 32 (2020) 1101–1110, https://doi.org/10.1021/acs.chemmater.9b03933.

[28] T.A. Hales, K.T. Moller, T.D. Humphries, A.M. D'Angelo, C.E. Buckley, M. Paskevicius, Investigating the potential of alkali metal plumba-closo-dodecaborate $(B_{11}H_{11}Pb)^{2-}$ salts as solid-state battery electrolytes, J. Phys. Chem. C 127 (2023) 949–957, https://doi.org/10.1021/acs.jpcc.2c07226?urlappend=%3Fref%3DPDF&jav=VoR&rel=cite-as.

[29] Z. Lu, F. Ciucci, Metal borohydrides as electrolytes for solid-state Li, Na, Mg, and Ca batteries: a first-principles Study, Chem. Mater. 29 (2017) 9308–9319. https://pubs.acs.org/doi/10.1021/acs.chemmater.7b03284.

[30] A. Avelar, F.S. Tham, C.A. Reed, Superacidity of boron acids $H_2(B_{12}X_{12})$ (X=Cl, Br), Angew. Chem., Int. Ed. Engl. 48 (19) (2009) 3491–3493, https://doi.org/10.1002/anie.200900214.

[31] B. Gruner, J. Rais, P. Selucky, M. Lucanikova, Recent progress in extraction agents based on cobalt Bis(Dicarbollides) for partitioning of radionuclides from high-level nuclear waste, Boron Science: New Technologies and Applications, N. S. Hosmane (2011) 463–490, https://doi.org/10.1201/b11199, eISBN9780429062735.

[32] J. Fanfrlik, J. Brynda, J. Rezac, P. Hobza, M. Lepsik, Interpretation of Protein/Ligand crystal structure using QM/MM calculations: case of HIV-1 Protease/Metallacarborane complex, J. Phys. Chem. B 112 (2008) 15094–15102, https://doi.org/10.1021/jp803528w.

[33] R. Nnez, M. Tarres, A. Ferrer-Ugalde, F. FabriziDebiani, F. Teixidor, Electrochemistry and photoluminescence of icosahedral carboranes, boranes, metallacarboranes, and their derivatives, Chem. Rev. 116 (23) (2016) 14307–14378, https://doi.org/10.1021/acs.chemrev.6b00198.

[34] R.K. Roy, S. Krishnamurti, P. Geerlings, S. Pal, Local softness and hardness based reactivity descriptors for predicting Intra – and intermolecular reactivity sequences: carbonyl compounds, J. Phys. Chem. 102 (1998) 3746–3755, https://doi.org/10.1021/jp973450v.

[35] A. Aizman, R. Contreras, P. Pérez, Relationship between local electrophilicity and rate coefficients for the hydrolysis of carbenium ions, Tetrahedron 61 (2005) 889–895, https://doi.org/10.1016/j.tet.2004.11.014.

[36] C. Morell, A. Grand, A. Toro-Labbé, Theoretical support for using the Δf(r) descriptor, Chem. Phys. Lett. 425 (2006) 342–346, https://doi.org/10.1016/j.cplett.2006.05.003.

[37] C. Cárdenas, N. Rabi, P.W. Ayers, C. Morell, P. Jaramillo, P. Fuentealba, Chemical reactivity descriptors for ambiphilic reagents: dual descriptor, local hypersoftness and electrostatic potential, J. Phys. Chem. 113 (2009) 8660–8667, https://doi.org/10.1021/jp902792n.

[38] J. Padmanabhan, R. Parthasarathi, M. Elango, V. Subramanian, B. S. Krishnamoorthy, S. Gutierrez-Oliva, A. Toro-Labbe, D.R. Roy, P.K. Chattaraj, Multiphilic descriptor for chemical reactivity and selectivity, J. Phys. Chem. 111 (2007) 9130–9138, https://doi.org/10.1021/jp0718909.

[39] C. Morell, A. Grand, A. Toro-Labbé, New dual descriptor for chemical reactivity, J. Phys. Chem. 109 (2005) 205–212, https://doi.org/10.1021/jp046577a.

[40] G.I. Cárdenas-Jirón, S. Gutiérrez-Oliva, J. Melin, A. Toro-Labbé, Relations between potential energy, electronic chemical potential and hardness profiles, J. Phys. Chem. 101 (1997) 4621–4627, https://doi.org/10.1021/jp9638705.

[41] R.S. Mulliken, Molecular compounds and their spectra II, J. American Chem. Soc. 74 (3) (1952) 811–824, https://doi.org/10.1021/ja01123a067.
[42] T. Kar, S. Scheiner, A.B. Sannigrahi, Ab initio calculations of hardness and chemical potential of open shell systems using SCF, MP2 and MP4 methods, J. Mol. Struct.: THEOCHEM 427 (1998) 79–85, https://doi.org/10.1016/S0166-1280(97)00172-3.
[43] J. Luo, Z.Q. Xue, W.M. Liu, J.L. Wu, Z.Q. Yang, Koopmans' Theorem for large molecular systems within density functional theory, J. Phys. Chem. 110 (2006) 12005–12009, https://doi.org/10.1021/jp063669m.
[44] T. Gädt, J.-A. Dimmer, S. Fleischhauer, A. Frank, C. Nickl, T. Wutz, K. Eichele, L. Wesemann, Oxidation of germa- and stanna-*closo*-dodecaborate, Dalton Trans. 44 (2015) 4726–4731, https://doi.org/10.1039/C5DT00099H.
[45] V. Brindha, B.S. Krishnamoorthy, Isomer preferences and structural studies on cobaltaboranes – a theoretical investigation, BiointerfaceReseach in Applied Chemistry 14 (3) (2024) 73, https://doi.org/10.33263/BRIAC143.073.
[46] V. Nagalakshmi, R. Nandhini, V. Brindha, B.S. Krishnamoorthy, K. Balasubramani, Half-sandwich ruthenium(II) complexes containing biphenylamine based Schiff base ligands: synthesis, structure and catalytic activity in amidation of various aldehydes, J. Organomet. Chem. 912 (2020) 121175, https://doi.org/10.1016/j.jorganchem.2020.121175.
[47] S. Gomathi, K. Kavitha, N. Savitha, A. Mohana, V. Brindha, B.S. Krishnamoorthy, Molecular structure, reactivity and spectroscopic properties of Hallucinogens Psilocybin, mescaline and their Derivatives–A computational Study, Lett. Appl. Nano. Bio. Sci. 12 (2022) 105, https://doi.org/10.33263/LIANBS124.105.
[48] Yusuf Sert, Mustafa R. Albayati, Fatih Şen, Necmi Dege, The DFT and in-silico analysis of 2,2′-((1e,1′e)-((3,3′-dimethyl-[1,1′-biphenyl]−4,4′ diyl)bis (azanylylidene))bis(methanylylidene))diphenol molecule, Colloids Surf. A Physicochem. Eng. Asp. 687 (2024) 133444, https://doi.org/10.1016/j.colsurfa.2024.133444.
[49] Necmi Dege, Halil Gökce, Onur Erman Doğan, Gökhan Alpaslan, Tuğgan Ağar, S. Muthu, Yusuf Sert, Quantum computational, spectroscopic investigations on N-(2-((2-chloro-4,5-dicyanophenyl)amino)ethyl)-4-methylbenzenesulfonamide by DFT/TD-DFT with different solvents, molecular docking and drug-likeness researches, Colloids Surf. A Physicochem. Eng. Asp. 638 (2022) 128311, https://doi.org/10.1016/j.colsurfa.2022.128311.
[50] Mahmood A. Albo Hay Allah, Asim A. Balakit, Hamida Idan Salman, Ahmed Abdulridha Ali, Yusuf Sert, New heterocyclic compound as carbon steel corrosion inhibitor in 1 M H_2SO_4, high efficiency at low concentration: experimental and theoretical studies, J. Adhes. Sci. Technol. 37 (3) (2022) 525–547, https://doi.org/10.1080/01694243.2022.2034588.
[51] F. Neese, Software update: the ORCA program system—Version 5.0, WIREs Comput. Mol. Sci. 12 (2022) e1606, https://doi.org/10.1002/wcms.1606.
[52] S.H. Vosko, L. Wilk, M. Nusair, Accurate spin-dependent electron liquid correlation energies for local spin density calculations: a critical analysis, Can. J. Phys. 58 (1980) 1200–1211, https://doi.org/10.1139/p80-159.
[53] A.D. Becke, Density functional calculations of molecular bond energies, J. Chem. Phys. 84 (1986) 4524–4529, https://doi.org/10.1063/1.450025.
[54] A.D. Becke, Density- functional exchange-energy approximation with correct asymptotic behavior, Phys. Rev. 38 (1988) 3098–3100, https://doi.org/10.1103/PhysRevA.38.3098.
[55] J.P. Perdew, Density-functional approximation for the correlation energy of the inhomogeneous electron gas, Phys. Rev. B 33 (1986) 8822–8824, https://doi.org/10.1103/PhysRevB.33.8822.
[56] B.S. Krishnamoorthy, A. Thakur, K.K.V. Chakrahari, S.K. Bose, P. Hamon, T. Roisnel, S. Kahlal, S. Ghosh, J.F. Halet, Theoretical and experimental investigations on hypoelectronic heterodimetallaboranes of Group 6 transition metals, Inorg. Chem. 51 (2012) 10375–10383, https://doi.org/10.1021/ic301571e.
[57] B.S. Krishnamoorthy, S. Kahlal, S. Ghosh, J.F. Halet, Electronic, geometrical and thermochemical studies on group-14 element-diruthenaborane cluster compounds: a theoretical investigation, Theor. Chem. Acc. 132 (2013) 1356, https://doi.org/10.1007/s00214-013-1356-6.
[58] K. Geetharani, B.S. Krishnamoorthy, S. Kahlal, S.M. Mobin, S. Ghosh, J.F. Halet, Synthesis and characterization of HypoelectronicTantalaboranes: comparison of geometric and electronic structures of $[(Cp^*TaX)_2B_5H_{11}]$ (X = Cl, Br, I), Inorg. Chem. 51 (2012) 10176–10184, https://doi.org/10.1021/ic300848f.
[59] F. Weigend, R. Ahlrichs, Balanced basis sets of split valence, triple zeta valence and quadruple zetavalence quality for H to Rn: design and assessment of accuracy, Phys. Chem. Chem. Phys. 7 (2005) 3297, https://doi.org/10.1039/b508541a.
[60] S. Grimme, J. Antony, S. Ehrlich, H. Krieg, A consistent and accurate *ab initio* parametrization of density functional dispersion correction (DFT-D) for the 94 elements H-Pu, J. Chem. Phys. 132 (2010) 154104, https://doi.org/10.1063/1.3382344.
[61] S. Grimme, S. Ehrlich, L. Goerigk, Effect of the damping function in dispersion corrected density functional theory, J. Comput. Chem. 32 (2011) 1456–1465, https://doi.org/10.1002/jcc.21759.
[62] E.R. Johnson, A.D. Becke, A post-hartree-fock model of intermolecular interactions: inclusion of higher-order corrections, J. Chem. Phys. 124 (2006) 174104, https://doi.org/10.1063/1.2190220.
[63] E.R. Johnson, A.D. Becke, A post-hartree-fock model of intermolecular interactions, J. Chem. Phys. 123 (2005) 024101, https://doi.org/10.1063/1.1949201.
[64] J. Mareš, J. Vaara, *Ab initio* paramagnetic NMR shifts *via* point-dipole approximation in a large magnetic-anisotropy Co(II) complex, Phys. Chem. Chem. Phys. 20 (2018) 22547–22555, https://doi.org/10.1039/C8CP04123G.
[65] Z.S. Safi, N. Wazzan, DFT calculations of ^{1}H and ^{13}C-NMR chemical shifts of 3-methyl-1-phenyl-4-(phenyldiazenyl)-1H-pyrazol-5-amine in solution, Sci. Rep. 12 (2022) 17798, https://doi.org/10.1038/s41598-022-22900-y.
[66] E.D. Becker, High Resolution NMR: Theory and Chemical Applications, third ed., 2000, https://doi.org/10.1016/B978-0-12-084662-7.X5044-3. ISBN: 9780120846627.
[67] P.K. Chattaraj, B. Maiti, U. Sarkar, Philicity: a unified treatment of chemical reactivity and selectivity, J. Phys. Chem. 107 (2003) 4973–4975, https://doi.org/10.1021/jp034707u.
[68] D.R. Roy, R. Parthasarathi, J. Padmanabhan, U. Sarkar, V. Subramanian, P. K. Chattaraj, Careful scrutiny of the philicity concept, J. Phys. Chem. 110 (2006) 1084–1093, https://doi.org/10.1021/jp053641v.
[69] W. Tiznado, O.B. Oña, V.E. Bazterra, M.C. Caputo, J.C. Facelli, M.B. Ferraro, P. Fuentealba, Theoretical study of the adsorption of H on Si_n clusters (n= 3-10), J. Chem. Phys. 123 (2005) 214301, https://doi.org/10.1063/1.2128675.
[70] E. Osorio, M.B. Ferraro, O.B. Oña, C. Cardenas, P. Fuentealba, W. Tiznado, Assembling small silicon clusters using criteria of maximum matching of the Fukui functions, J. Chem. Theor. Comput. 7 (12) (2011) 3995–4001, https://doi.org/10.1021/ct200643z.
[71] O. Yañez, R. Báez-Grez, D. Inostroza, R. Pino-Rios, W.A. Rabanal-León, J. Contreras-García, C. Cardenas, W. Tiznado, Kick–Fukui: a Fukui function-guided method for molecular structure prediction, J. Chem. Inf. Model. 61 (8) (2021) 3955–3963, https://doi.org/10.1021/acs.jcim.1c00605.
[72] E. Osorio, A.P. Sergeeva, J.C. Santos, W. Tiznado, Theoretical study of the $Si_{5-n}(BH)_n^{2-}$ and $Na(Si_{5-n}(BH)_n)^-$ (n = 0–5) systems, Phys. Chem. Chem. Phys. 14 (2012) 16326–16330, https://doi.org/10.1039/C2CP42674A.
[73] Lars Wesemann, UlliEnglert, the first *closo*-monosilaborane, Angew. Chem. 108 (1996) 586–587, https://doi.org/10.1002/anie.199605271.
[74] Torben Gadt, Lars Wesemann, Stanna-*closo*-dodecaborate: the Crystal Structure of $[Li(thf)_3]_2[SnB_{11}H_{11}]$, Vibrational Spectroscopy, Thermal Analysis and DFT CalculationsZeitschrift fur Anorganische und AllgemeineChemie, Z. Anorg. Allg. Chem. 633 (2007) 693–699, https://doi.org/10.1002/zaac.200600348.
[75] F.H. Allen, O. Kennard, D.G. Watson, L. Brammer, A.G. Orpen, R. Taylor, Tables of bond lengths determined by X-ray and neutron diffraction. Part 1. Bond lengths inorganic compounds, J. Chem. Soc, Perkin. Trans. 2S1 (1987), https://doi.org/10.1039/p298700000s1.
[76] Lars Wesemann, Michael Trinkaus, UlliEnglert, Jens Muller, Silaborates with an unprecedented cluster geometry, Organometallics 18 (1999) 4654–4659, https://doi.org/10.1021/om9903994.
[77] Yuzhong Wang, Pingrong Wei YaomingXie, R. Bruce King, Henry F. Schaefer III, R. Schleyer Paul von, Gregory H. Robinson, A stable Silicon(0) compound with a si=si double bond, Science 321 (2008) 1069, https://doi.org/10.1126/science.1160768.
[78] M.J. Fink, M.J. Michalczyk, K.J. Haller, J.W.R. Michl, X-ray crystal structures for two disilenes, Organometallics 3 (1984) 793–800, https://doi.org/10.1021/om00083a025.
[79] T. Sasamori, J.S. Han, K. Hironaka, N. Takagi, S. Nagasw, N. Tokitoh, Synthesis and structure of stable 1,2-diaryldisilyne, Pure Appl. Chem. 82 (2010) 603–612, https://doi.org/10.1351/PAC-CON-09-08-02.
[80] L.V. Ya, T. Fukawa, M. Nakamoto, A. Sekiguchi, T.L. Boris, M. Karni, Y. Apeloig, (*t*Bu2MeSi)2*Sn*=*Sn*(*SiMetBu2*)2 : A Distannene with a >Sn=Sn< Double Bond That is Stable Both in the Solid State and in Solution, J. Am. Chem. Soc. 128 (35) (2006) 11643–11651, https://doi.org/10.1021/ja063322x.
[81] K.W. Klinkhammer, M. Niemeyer, J. Klett, Chem. Eur J. 5 (1999) 2531, https://doi.org/10.1002/(SICI)1521-3765(19990903)5:9%3C2531::AID-CHEM2531%3E3.0.CO;2-2.
[82] K. Wade, Structural and bonding patterns in cluster chemistry, Adv. Inorg. Chem. Radiochem. 18 (1976) 1–66, https://doi.org/10.1016/S0065-2792(08)60027-8.
[83] K. Wade, The structural significance of the number of skeletal bonding electron-pairs in carboranes, the higher boranes and borane anions, and various transition-metal carbonyl cluster compounds, J. Chem. Soc. D Chem. Commun. 15 (1971) 792–793, https://doi.org/10.1039/C29710000792.
[84] D.M.P. Mingos, A general theory for cluster and ring compounds of the main group and transition elements, Nat. Phys. Sci. (Lond.) 236 (1972) 99–102, https://doi.org/10.1038/physci236099a.
[85] Jaromir Plesek, Tomas Jelinek, Eva Drdakova, BohumilStibr StanislavHermanek, A convenient preparation of 1-$CB_{11}H_{12}$ and its c-amino derivatives, Chem. Commun. 49 (1984), https://doi.org/10.1135/cccc19841559.
[86] Lauri Toom, Agnes Kutt, Ivo Leito, Simple and scalable synthesis of the carborane anion $CB_{11}H_{12}$, dalton, OR Trans. 48 (2019) 7499–7502, https://doi.org/10.1039/C9DT01062A.